ELSEVIER

Chemical Geology 167 (2000) 53–63

CHEMICAL GEOLOGY
INCLUDING
ISOTOPE GEOSCIENCE

www.elsevier.com/locate/chemgeo

In situ time-resolved X-ray diffraction of iron sulfides during hydrothermal pyrite growth

C.L. Cahill [a,*], L.G. Benning [b,1], H.L. Barnes [b], J.B. Parise [a,c]

[a] *Department of Chemistry, State University of New York, Stony Brook, NY 11794, USA*
[b] *Department of Geosciences, Penn State University, University Park, PA 16802, USA*
[c] *Department of Geosciences, State University of New York, Stony Brook, NY 11794, USA*

Abstract

Pyrite formation under hydrothermal conditions has been studied using in situ time-resolved X-ray diffraction (XRD). This study employed two different synchrotron X-ray sources (National Synchrotron Light Source (NSLS), Advanced Photon Source (APS); Brookhaven and Argonne National Laboratories, USA, respectively) and two types of reaction cells (capillary and hydrothermal autoclave type) to examine reactions in the Fe–S system under both anoxic and controlled oxic conditions. Starting materials were mackinawite slurries equilibrated in reduced, $H_2S_{(aq)}$ solutions and heated to a maximum of 190°C. The results show that under fully anoxic conditions, mackinawite persists to at least 120°C, while aerated (oxic) slurries transform rapidly to greigite, pyrite, magnetite and goethite. Possible reaction mechanisms are discussed in light of these results. These experiments are the first application of previously described in situ reaction cells to anoxic and oxic reactions in the Fe–S system. Finally, the capabilities of each cell type and their applicability to other systems are discussed.

Keywords: In situ; X-ray; Pyrite; Hydrothermal; Mackinawite

1. Introduction

Pyrite formation processes are still not completely understood despite their importance in several geochemical cycles. It is generally accepted that the first step in its formation at temperatures below 300°C is the nucleation of a short-range-ordered ferrous monosulfide that is a precursor to mackinawite (Fe_9S_8) (Davison, 1991; Schoonen and Barnes, 1991b; Parise et al., 1994; Rickard, 1995). The chemical composition of this initial precipitate varies from $Fe_{0.87}S$ to $FeS_{1.1}$ (Berner, 1964; Rickard, 1969, 1975; Sweeney and Kaplan, 1973), however here, we will refer to this phase as mackinawite, nominally FeS. Mackinawite may be a precursor to greigite (Fe_3S_4), which can then convert to pyrite (FeS_2). Numerous experimental studies have examined these nucleation and transformation reactions, yet have failed to yield a universally accepted pathway and mechanism (Berner, 1970; Rickard, 1975; Taylor et al., 1979b; Luther, 1991; Schoonen and Barnes, 1991a,b; Wilkin and Barnes, 1996). The absence of such a scheme is partially due to difficulties arising

* Corresponding author. Present address: Department of Civil Engineering and Geological Sciences, University of Notre Dame, Notre Dame, IN 46556 USA.
E-mail addresses: christopher.cahill@sunysb.edu, ccahill@nd.edu (C.L. Cahill).
[1] Present address: School of Earth Sciences, University of Leeds, Leeds, LS 2 9 JT, UK.

0009-2541/00/$ - see front matter
PII: S0009-2541(99)00199-0

from oxidation state changes in both crystalline and aqueous phases present during the transformation. These studies have indicated however, that the conversion of mackinawite to pyrite is an oxidation process, although the oxidant remains in question.

Three primary pathways have been proposed: the first is a progressive sulfidation and conversion of iron monosulfides to pyrite (Berner, 1967, 1970; Rickard, 1969; Schoonen and Barnes, 1991a); varieties of the first are:

$$FeS(s) + S^{o}(s) \rightarrow FeS_2(s) \quad (1)$$

$$FeS(s) + S_n^{2-} \rightarrow FeS_2(s) + S_{n-1}^{2-} \quad (1a)$$

where FeS represents an iron monosulfide such as the short-range-ordered mackinawite, mackinawite or greigite. The sulfur source might be either elemental (S^o), or a species of intermediate oxidation state (S_n^{2-}, polysulfide, etc.). The FeS to FeS_2 transformation should be favored by a redox reaction between the intermediate sulfur source and the reduced iron in the monosulfide. In addition, this route includes the formation of the mixed valence (Fe^{2+}/Fe^{3+}) phase greigite prior to the formation of pyrite. Both of these reactions, however, are hindered by armoring caused by the increase in molar volumes between the solid reactants and products (Furukawa and Barnes, 1995).

The above reactions are written in terms of sulfur addition. This is often done because several different sulfur species have been shown to react with the monosulfides (Luther, 1991; Schoonen and Barnes, 1991b; Wei and Osseo-Asare, 1995; Wilkin and Barnes, 1996). The transformation to pyrite can, however, be written in terms of an iron loss mechanism, the second pathway:

$$2FeS + 2H^{+} \rightarrow FeS_2 + Fe^{2+} + H_2(g) \quad (2)$$

Such a reaction was suggested by Berner (1970), and examined further by Schoonen and Barnes (1991b), Furukawa and Barnes (1995), and most recently, by Wilkin and Barnes (1996). Furukawa and Barnes (1995) showed that a decrease in the molar volume of solids promoted the transformation, while Wilkin and Barnes (1996) gave isotopic evidence that the various sulfur sources contributed no sulfur to the resulting pyrite and demonstrated that Fe-loss was the correct mechanism.

A third proposed pathway by which iron monosulfides transform to pyrite is via the H_2S route (Taylor et al., 1979b; Wächtershäuser, 1988; Drobner et al., 1990; Rickard, 1997) in which H_2S is the oxidant:

$$FeS + H_2S \rightarrow FeS_2 + H_2(g) \quad (3)$$

This reaction has been employed to explain the formation of pyrite in presumably anaerobic environments. This process, however, again implies an improbable increase in molar volume (Furukawa and Barnes, 1995).

These proposed mechanisms are investigated here via time-resolved in situ X-ray diffraction (XRD). The impetus for such experiments is the ability of in situ XRD (under hydrothermal conditions) to monitor the course of this transformation without compromising the reaction conditions; i.e., no sampling or quenching is necessary to obtain diffraction data. The sample cells used permit careful control of the reaction environment (temperature, oxygen level, pH, etc.), and thus allow study of systems under a variety of well-controlled reaction conditions. In addition, monochromatic studies can produce data of sufficient quality for Rietveld structural analyses (Rietveld, 1969; Norby, 1997b), making this technique potentially attractive to a wide range of scientists. Recent applications of in situ XRD have included studies of cement during hardening (Shaw et al., this issue (a)) growth of zeolites and other microporous materials (Norby, 1997a; Cahill et al., 1998; Christensen et al., 1998; Francis and O'Hare, 1998), ion exchange (Lee et al., 1998), gas sorption (Grey et al., 1997), solid state phase transitions with pressure and temperature (Cruciani et al., 1997; Parise et al., 1998) as well as a host of other reaction types (Wilkinson et al., 1994; Price et al., 1996; Cheetham and Mellot, 1997).

A recent investigation by Lennie et al. (1997) examined the solid state phase transition of mackinawite to greigite. Their experiments demonstrated the utility of in situ XRD as a structural probe in suggesting a crystal chemical transformation mechanism. While the apparatus for this study was appropriate for the investigation of the solid state phase transition, a full examination of the reaction sequence under controlled hydrothermal conditions was not possible.

In the current study, in situ diffraction techniques have been employed to examine the path and mechanism of the conversion of mackinawite to pyrite under hydrothermal conditions, both aerobically and anaerobically. This application extends the role of in situ XRD to include primarily chemical and pathway information. Rather than a full structural or crystal chemical investigation, reported here is an application of previously described experimental apparatus to: (1) test the suggested mackinawite to pyrite conversion sequence and (2) examine the role of oxygen in this process.

2. Experimental section

2.1. Apparatus

Two different synchrotron sources and two types of reaction cells were used to study the formation and reactions of solids in the Fe–S system under hydrothermal conditions. The experiments were designed to explore the possibilities and limitations of carrying out in situ X-ray experiments under anoxic and controlled oxic conditions using in situ and ex situ injection techniques. The first set of experiments (Table 1) were conducted at beamline 13-BMD of the GeoSoilEnviro Consortium for Advanced Radiation Science (GSE-CARS) at the Advanced Photon Source (APS) of Argonne National Laboratory. The beamline set up at this station consists of a series of pre-sample slits that reduce the size of the incident X-ray beam to 200×50 μm. After encountering the sample, the diffracted X-rays are collected via a brass collimator with a 500-μm slit width into a 2400 channel, energy dispersive single element Canberra detector. The detector angle was optimized to $4.5°$ 2θ to include the maximum number of peaks from materials in the Fe–S system while minimizing the effects of the sample holder and reaction vessel. A more detailed description of the facilities at the APS can be found in Rivers et al. (1998).

The reaction cell shown in Fig. 1 was designed and commissioned previously by Evans et al. (1994) and is composed of a stainless steel Parr® reaction vessel (25 ml) with a section of its wall milled down to a thickness of 0.4 mm. This thinner portion of the wall permits transmission of white X-radiation and has a maximum operating temperature of 230°C. Attached to the top of the cell is a head consisting of a pressure transducer, safety relief valve and an injection reservoir (2 ml). The injection reservoir consists of a remotely controlled gate valve that is activated via an overpressure of an inert gas (CO_2). This permits injection of a second solution into the cell at controlled time and temperature conditions. The cell was placed in a notched aluminum block that is heated by four resistance cartridge heaters. The temperature was monitored with K-type thermocouples in contact with the outside of the reaction vessel and was controlled to ± 5°C. Data collection proceeded during the entire course of the experiment and recorded a full spectrum every 3 min. Data were extracted and processed via an in-house-produced Interactive Data Language[2] (IDL®) routine.

Initial runs were conducted with an anoxic, ex situ prepared, low pH Fe/H_2S solution that was loaded into the cell (Fig. 1) under a constant flow of ultra-high purity nitrogen. The cell was previously purged via N_2 and all transfers were done via syringes. At this pH, little precipitate is present due to the high solubility of FeS. The injection reservoir was filled under equally anoxic conditions with a freshly prepared oxygen-free 1.0 N NaOH solution. The cell was sealed, inserted in the heater and brought to temperature. Subsequently, the NaOH solution from the reservoir was injected via the remotely controlled valve initiating the precipitation of iron monosulfide phase. Only weak diffraction peaks were observed from this sample, as the resulting slurry was not of sufficient density to produce a satisfactory diffraction signal. Due to these experimental difficulties, the injection procedure was abandoned and the mixing was performed ex situ forming a colloidal suspension, which was filtered and the solids transferred (as a wet paste) to the reaction cell. This new procedure however, compromised the anoxic conditions (see below).

The second set of experiments were performed at beamline X7B of the National Synchrotron Light Source (NSLS) at Brookhaven National Laboratory using monochromatic radiation. For this study, the

[2] IDL is a registered trademark of Research Systems, 2995 Wilderness Place, Boulder, CO 80301, USA.

Table 1
Summary of experimental conditions
Arrow implies ''replaced by...''

Run number	pH	Reaction conditions[a]	Products[b]
APS-SB5	3.91	Oxic; $T = 80$°C; 5 h	Mk → insufficient density
APS-SB7	3.91	Oxic; $T = 130$°C to 190°C; 4 h	Gr, Py, He
APS-SB8	3.50	Anoxic/oxic; $T = 41$°C to 180°C 3.75 h	Gr, Py
NSLS-SB101	3.64	Anoxic; $T = 120$°C 4 h	Mk, (trace Goe); Fig. 4.
NSLS-103	3.64	Mixed N_2/O_2 overpressure; $T = 120$°C; 1 h	Mk, Goe
NSLS-106b	3.64	O_2 over-pressure; $T = 120$°C; 2 h	Mk → Gr,Goe
NSLS-111	3.64	Aerated slurry[c], $T = 150$°C; 1 h	Mk → Gr, Mgt
NSLS-SB11	4.50	Anoxic; $T = 150$°C; 3 h	Mk, Gr
NSLS-SB14	4.50	Aerated slurry (20 min); $T = 250$°C; 1 h	Mk → Gr, Goe
NSLS-SB16	4.50	Aerated slurry (50 min); $T = 150$°C; 2.5 h	Mk → Gr, Py, Mgt, (trace Goe), S?; Fig. 5.

[a]All saturated with 100% H_2S (0.1 m, 1 bar).
[b]Gr = greigite, Py = pyrite, Mk = mackinawite, Mgt = magnetite, He = hematite, Goe = goethite, S = sulfur.
[c]Exploratory run, aeration time not known precisely.

beamline set up was as follows: incident white radiation was selected via 2 Si (111) monochrometers to a desired wavelength (0.890 or 1.095 Å) as determined from a unit cell refinement of LaB_6 (NIST

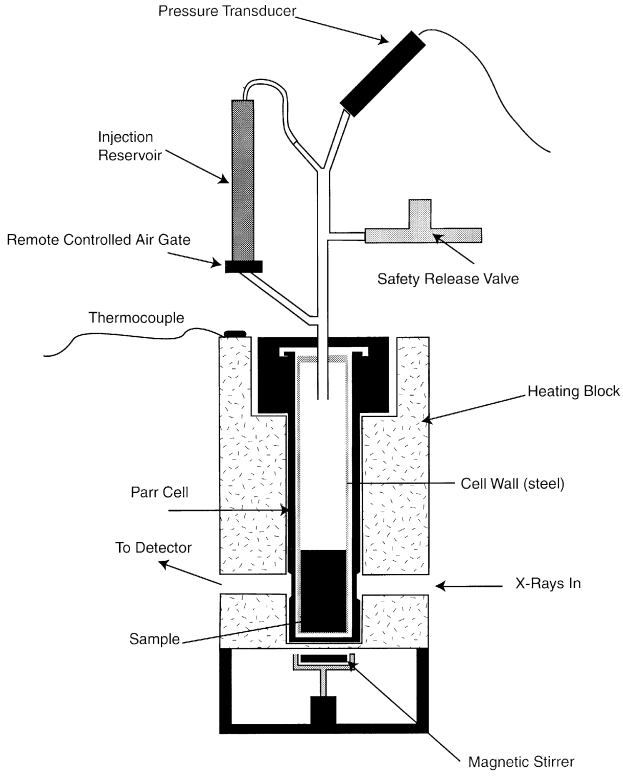

Fig. 1. The hydrothermal autoclave type reaction cell as described by Evans et al., 1994. (Figure modified after Shaw et al., 1998 and Shaw et al., this issue (a)) Shown as used at the APS. Reactions take place in a stainless steel Parr® bomb that has been machined to allow transmission of white X-rays. Temperature control is through a copper resistance heating block, while an injection reservoir can introduce reactants to the experiment at various times via a remotely controlled gate valve.

SRM660a). The size of the incident beam was controlled via two upstream slits to be 1.0×0.5 mm. The sample cell (Fig. 2 and below) was affixed to a horizontally mounted Huber four-circle goniometer, and diffracted X-rays were collected on a translating imaging plate (TIP) system. Further details of the experimental set up at X7B have been reported previously (Gualtieri et al., 1996).

The sample cell (Fig. 2) has been described in detail elsewhere (Norby, 1996, 1997a; Cahill et al., 1998), and only a brief description will be given here. Ex situ prepared sample slurries were loaded under flowing oxygen-free nitrogen into a 0.7-mm quartz capillary (A) closed at one end (Fig. 2). The horizontally mounted capillary is held in place with a Swagelock® (B) fitting mounted on a modified goniometer head. Hydrothermal conditions were obtained via an air heater and pressure was maintained inside the capillary with an overpressure of N_2 gas applied to the open end of the capillary (optionally, N_2 can be replaced with O_2 or any desired gas). A full diffraction pattern is collected on a portion (C) of the imaging plate (IP) that is defined by two lead shields (D). The IP is translated (along arrow (E)) to expose fresh portions of the plate and obtain diffraction data as a function of time. At the conclusion of a run, the exposed plates are read on a Fuji BAS2000 scanner and the data are extracted using IDL® routines. Peak identification via the Powder Diffraction File (PDF) entries was possible by extracting slices of the time-resolved data and stacking them against the card for each phase. Time resolution for these experiments is 5 min or less. Using this technique, two types of experiments were carried out: anoxic and controlled oxic runs as explained below.

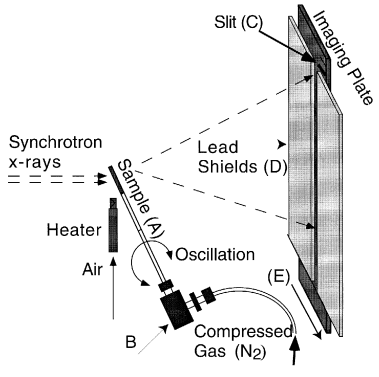

Fig. 2. The capillary reaction cell and translating IP detection system as used at the NSLS (Norby, 1996). Hydrothermal conditions are maintained in a horizontally mounted 1.0-mm quartz capillary via an overpressure of $N_{2(g)}$ and an air heater. Monochromatic diffraction spectra are collected on a photostimulable translating imaging plate mounted perpendicular to the capillary. The direct beam is offset (vertically) from the center of the IP to allow collection of a full diffraction pattern.

2.2. Starting material: preparation and analysis

The steps for preparing and handling the samples prior to in situ X-ray data collection are similar to the ones described in detail in the complementary paper in this issue (Benning et al., this issue); given here is only a brief summary and differences in methodology imposed by individual experiments. All experiments, unless otherwise mentioned, were carried out under carefully controlled oxygen-free conditions. Particular care was taken during preparation and transfer of solutions between the steps of each experiment. All chemicals and gases (except N_2) used were reagent grade. Oxygen-free nitrogen was produced by passing nitrogen gas of ultra high purity through an additional oxygen scrubber (Alltech®). This gas was used in all experiments where anoxic conditions were intended.

Starting solutions were prepared from ferrous ammonium sulfate salt mixed with freshly boiled and under oxygen-free N_2-cooled doubly distilled water. This solution was equilibrated with 100% H_2S gas at 1 bar, achieving a saturated (i.e., 0.1 m H_2S), reduced, low-pH solution. The precipitation of iron monosulfides was induced (except in the initial runs at APS) by injecting a known amount of oxygen-free 1.0 N NaOH into the reactor, i.e., increasing the pH of the solution and decreasing the solubility of iron monosulfide. The composition and morphology of the starting solids were checked with conventional XRD (Rigaku Geigerflex, Cu$K\alpha$ radiation, scanning rate of 2°/min for the 2θ range 5–65°) and scanning electron microscopy with an energy dispersive system (SEM–EDS, Phillips XL-20). The pH of the starting solutions was measured at 25°C using a sulfide- tolerant glass combination electrode (Corning®) calibrated against NIST-traceable buffer solutions.

The initial experiments carried out at APS were designed such that injection of the oxygen-free NaOH

was done on-line as described above. The final runs, however, were carried out with ex situ prepared iron monosulfide suspensions filtered oxically, thus compromising the intended anoxic conditions. As expected, fast transformation of the initial iron monosulfide precipitate was observed at the start of the real time X-ray experiment. For the NSLS runs, the ex situ prepared solutions were decanted under controlled anoxic conditions and filled (via ultra-fine syringes, from the bottom up to replace gas space) into capillaries that were sealed under nitrogen. For controlled oxic experiments, air was bubbled through the decanted slurries for a fixed amount of time before the in situ measurements (Table 1).

3. Results

3.1. APS; oxic conditions

After several trials of oxygen-free, NaOH solution injections as described above, the resulting reaction slurry was found to be of insufficient density to provide an adequate diffraction signal. In order to increase sample density, injections were carried out off-line in a glass reaction vessel (Benning et al., this issue). The suspension was filtered and the solids then transferred (via syringe) to the reaction cell (Fig. 1) under flowing N_2. After sealing, the cell was loaded into the heating block at an initial temperature of 41°C. The temperature was increased to 110°C over 50 min, held for 160 min and finally ramped to 185°C over 30 min. Fig. 3 is a plot of the resulting time resolved diffraction spectra collected at beamline 13-BMD at the APS (run # SB8 in Table 1). The initial portion of the experiment (0 to 75 min) exhibits only weak diffraction peaks from the sample; strong peaks at approximately 60 keV are due to diffraction of the steel cell itself. Difficulties in peak assignment are compounded by significant overlap in this region. The large background hump from approximately 14 to 58 keV is the result of X-ray scatter off the reaction vessel and fluid present in the sample. The sample density during the

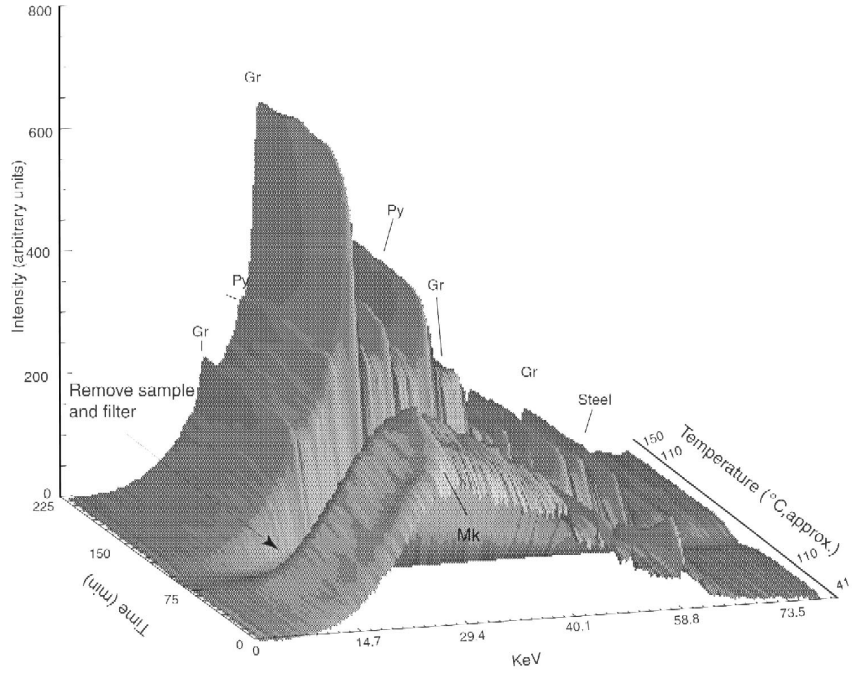

Fig. 3. Time-resolved plot of diffraction data obtained in the autoclave-type cell (Fig. 1). Run APS-SB8. At the beginning of the reaction, only weak diffraction peaks from the sample (mackinawite, Mk) were observed. After pausing to filter the reactants and increase the sample density, the anoxic conditions were compromised and the onset of greigite (Gr) and pyrite (Py) is clearly visible.

early portion of the run was again too low to produce a sufficient diffraction signal. This prompted interruption of the experiment (at approximately 75 min; Fig. 3) in order to filter the sample and further increase sample density. This process, however, compromised the anoxic nature of the reactants. After approximately 85 min, the sample was returned to the beam (at 110°C) as a thicker paste and the presence of greigite and pyrite became clearly visible under these slightly oxic conditions.

3.2. NSLS; anoxic conditions

In an effort to increase sample density and maintain oxygen-free conditions, similar experiments were conducted at beamline X7B of the NSLS using the reaction cell shown in Fig. 2. For this study, an ex situ prepared anoxic slurry (run # NSLS-SB101 in Table 1) was heated to 120°C over 30 min and held for 3.5 h. During this time, mackinawite is the only Fe–S phase observed (Fig. 4). A trace amount of goethite was noted and is likely the result of a reaction at the slurry/compressed N_2 interface due to impurities in the reagent grade overpressure gas or in surface contamination during cell loading and mounting.

3.3. NSLS; controlled oxic conditions

In order to promote the transformation of mackinawite to pyrite, the above experiment was repeated with an aerated starting material. Air was bubbled through a second ex situ prepared FeS slurry for 50 min (run # NSLS-SB16 in Table 1). After this treatment, the sample mixture was loaded into a capillary and heated to 150°C over 30 min and held for approximately 2 h. As expected, this oxygenated experiment shows the rapid disappearance of mackinawite followed by the appearance of greigite after approximately 30 min (Fig. 5). The onset of pyrite is observed at about 40 min, followed by the formation of magnetite at about 60 min. Goethite is present throughout almost the entire run. In the figure, the large increase in background scatter (as compared to Fig. 4) between 10° and 35° 2θ is due to the decrease in sample density after treatment with compressed air. The slurry was disturbed in the process and, due to time constraints, not allowed to settle

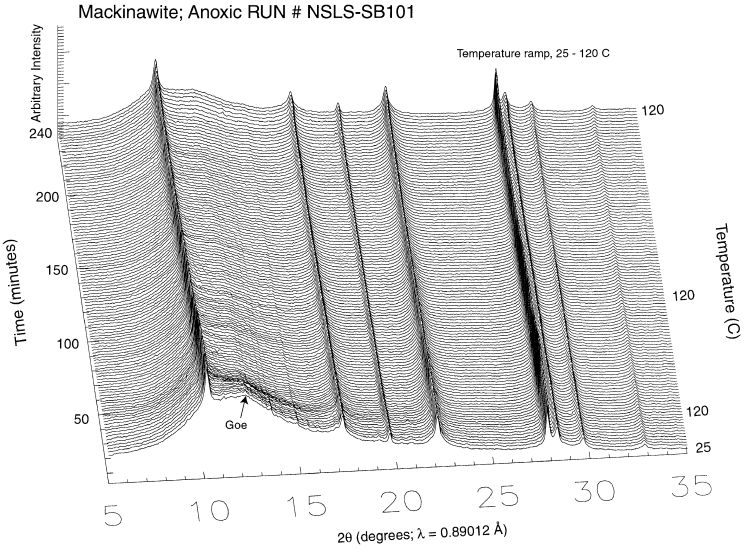

Fig. 4. Time-resolved spectra of an ex situ prepared anoxic slurry (run # NSLS-SB101 in Table 1) heated to 120°C as obtained in the capillary reaction cell (Fig. 2). Mackinawite (FeS) is the only iron sulfide phase observed after 3.5 h under these conditions (Goe = goethite).

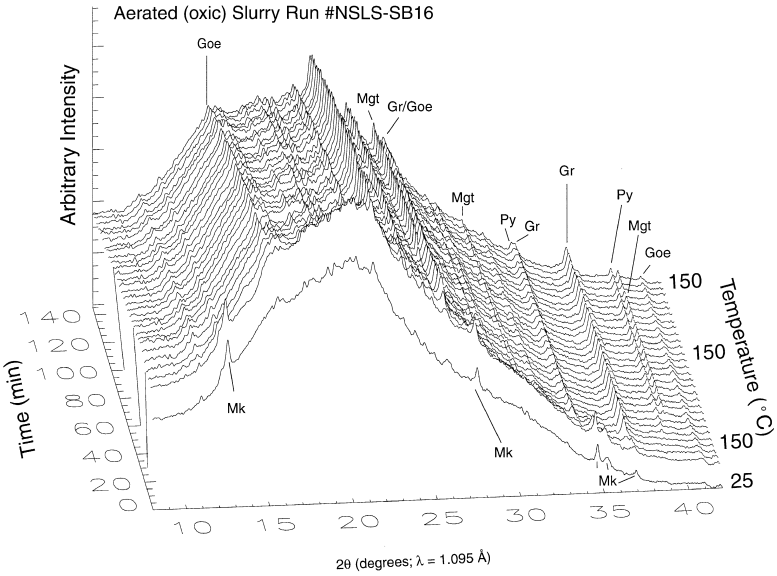

Fig. 5. Diffraction spectra of an ex situ prepared aerated slurry (NSLS-SB16, Table 1) heated to 150°C as obtained in the capillary reaction cell (Fig. 2). Note the rapid disappearance of mackinawite as it is replaced by greigite (Gr), goethite (Goe), pyrite (Py) and magnetite (Mgt) under these oxic conditions.

completely prior to loading for the in situ experiment. This scattering effect is similar to that observed in the APS experiments (Fig. 3).

4. Discussion

4.1. APS

The X-ray resolution obtained with the reaction cell in Fig. 1 was not well suited to these experiments, The low concentration of solids in the hydrothermal Fe−S slurry hindered production of a satisfactory diffraction signal. (This cell has been used in many other systems in which signal strength was not a problem — see, for example, Francis and O'Hare (1998).) Furthermore, the saturation limit of H_2S at 1 bar prevented the formation of a more concentrated reactant mixture. Since the reaction could not be performed under totally anoxic conditions, the data obtained (Fig. 3) cannot be interpreted with confidence and were thus not included in the conclusions (below). The slightly oxidized starting materials did, however, readily transform to pyrite under the conditions of this experiment. Such an observation is consistent with previously reported studies (e.g., Taylor et al., 1979a; Wilkin and Barnes, 1996; Benning et al., this issue).

4.2. NSLS

It has been shown in previous studies at temperatures below 100°C, that without oxygen, mackinawite will remain stable in reduced H_2S solutions (Berner 1967; Rickard 1969, 1975; Roberts et al., 1969; Taylor et al., 1979a; Wilkin and Barnes 1996; Benning et al., this issue). In the current study, this is confirmed: mackinawite is stable to at least 120°C in a reduced H_2S environment. This finding suggests that the proposed mechanism of fast iron monosulfide conversion to pyrite via the H_2S pathway (Eq. (3)) is not effective at the reported rate by (Rickard 1997; pyrite formed under similar conditions within 1 h). The current anoxic experiments show that mackinawite is the only sulfide phase observed after 3.5 h (Fig. 4). In contrast, during oxic experiments, the formation of greigite and pyrite as well as goethite and magnetite was observed (Fig. 5). There is little evidence of the formation of elemental sulfur in these experiments. If present, it is expected to be a minor phase and the strongest diffraction peaks lie in

regions of high background and obscure peak assignment. In run NSLS-SB16 (Table 9, Fig. 5), however, weak features corresponding to PDF numbers 080247 (α-sulfur) and 201225 (sulfur) are noted. This is consistent with observations made under similar conditions at lower temperatures by Benning et al. (this issue). Typically, XRD of solid samples at a synchrotron source can detect less than 1.0% (by weight) of a secondary phase. For these experiments, that value is compromised due to interference from water within the samples and the steel sample cell itself. A conservative estimate is that 5% (wt.) is necessary for detection.

Previous 'intentional' oxidation experiments were reported by Taylor et al. (1979a). They noted that mackinawite samples exposed to air for ''as little as a few minutes,'' reacted quite differently with H_2S; presumably due to surface oxidation. Wilkin and Barnes (1996) showed that air-exposed FeS converted to pyrite at a much faster rate than non-exposed samples. In addition, they reported that when unoxidized FeS was reacted with oxygen (their runs 16 and 17), the transformation to pyrite yielded the highest conversion rates. Benning et al. (this issue) also show that intentional oxidation (either of the solution and/or the precursor solid surface) drove the reaction at a much faster rate while unoxidized samples remained stable. Such surface oxidation may also explain why pyrite is observed in experiments by Drobner et al. (1990) and Rickard (1997) under presumably anoxic conditions. Taylor et al. (1979a) also noted that at 160°C, the conversion of monosulfide to pyrite in anoxic experiments, proceeded much faster than below 100°C, possibly indicating an upper limit of the thermal stability of mackinawite. In a forthcoming paper, however, recent experiments have shown that mackinawite might persist to at least 180°C (Benning et al., 1999, in preparation).

5. Conclusions

The results of in situ XRD experiments on Fe–S under hydrothermal conditions suggest that the transformation sequence: mackinawite → greigite → pyrite is observed only when oxidation is induced. Fe–S slurries under reduced, anoxic (H_2S) conditions contain mackinawite as the only iron sulfide phase, while controlled aerobic conditions induce changes in oxidation state in both the liquid and solid phases and promote the mono- to disulfide transformation.

This study forms the basis of a more thorough investigation over a range of temperatures, pH conditions and starting materials, the results of which will allow construction of stability fields and acquisition of kinetic data. The challenges described herein regarding the exclusion of oxygen have demonstrated the need for modified reaction preparation and sample cells. Indeed, subtle shifts in oxygen level have shown significant changes in the mineralogy of this system. Careful control is therefore critical for this type of investigation. Recent and ongoing experiments using glass reaction cells and glove box techniques address this issue (Benning et al., in preparation).

The experimental techniques used in this study illustrate possible applications to a number of systems. The complementary nature of the reaction cells (real-time feedback and injection capabilities (Fig. 1) vs. improved sample density and Rietveld structure analysis (Fig. 2)) indicate the potential for thorough studies under a variety if conditions. In their current configurations, neither type of cell is particularly well suited to study the early stages of FeS nucleation reactions. Rather, other synchrotron-based techniques such as simultaneous SAXS/WAXS (small and wide angle X-ray scattering respectively) experiments may make a contribution to the study of these reactions (de Moor et al., 1997; Shaw et al., this issue (b)).

Acknowledgements

We thank the NSF (Grants DMR 97-13375 (JBP) and EAR-9526762 (HLB)) for financial support. Portions of this work were performed at GSE-CARS, Sector 13, APS at Argonne National Laboratory. GSE-CARS is supported by the National Science Foundation-Earth Sciences, Department of Energy-Geosciences, W.M. Keck Foundation and the United States Department of Agriculture. Use of the APS was supported by the US Department of Energy, Basic Energy Sciences, Office of Energy Research, under Contract No. W-31-109-Eng-38. The authors

are grateful to the beamline personnel including Mark Rivers, Nancy Lazars, Yanbin Wang, Guoyin Shen, Matt Newvile, Steve Sutton, Peter Eng and Mike Jagger. We also acknowledge Sam Shaw, Simon Clark and Mike Henderson of Daresbury Laboratory for the invitation to explore this system with their reaction cell.

Research carried out in part at the NSLS at Brookhaven National Laboratory is supported by the US Department of Energy, Division of Materials Sciences and Division of Chemical Sciences. Beamline X7B is supported under contract DE-AC02-98CH10886 with the US Department of Energy, Division of Chemical Sciences. We are grateful to Jonathan Hanson for assistance at the beamline and to Poul Norby whose contribution to the development of in situ measurements at X7B made these experiments possible. Numerous discussions with Rick Wilkin and Martin Schoonen have greatly improved the quality of this paper. C.L.C also wishes to thank the Mineralogical Society of America for a research grant in crystallography from the Edward H. Kraus Crystallographic Research Fund.

References

Benning, L.G., Cahill, C.L., Clark, S.M., Barnes, H.L., Parise, J.B., 1999. Mackinawite stability at high temperatures. In Proc. 9th V.M. Goldschmidt Conference, Lunar and Planetary Institute Contribution No. 971, pp. 24–25.

Benning, L.G., Wilkin, R.L., Barnes, H.L., this issue. Iron monosulfides and pyrite: in situ determination of formation pathways in reduced solutions.

Benning, L.G., Cahill, C.L., Clark, S.M., Parise, J.B., in preparation.

Berner, R.A., 1964. Iron sulfides formed from aqueous solution at low temperatures and atmospheric pressure. J. Geol. 72, 293–306.

Berner, R.A., 1967. Thermodynamic stability of sedimentary iron sulfides. Am. J. Sci. 265, 773–785.

Berner, R.A., 1970. Sedimentary pyrite formation. Am. J. Sci. 268, 1–23.

Cahill, C.L., Ko, Y., Hanson, J.C., Tan, K., Parise, J.B., 1998. Structure of microporous QUI-MnGS-1 and in situ studies of its formation using time resolved synchrotron X-ray powder diffraction. Chem. Mater. 10 (5), 1453–1458.

Cheetham, A.K., Mellot, C.F., 1997. In situ studies of the sol–gel synthesis of materials. Chem. Mater. 9, 2269–2279.

Christensen, A.N., Jensen, T.R., Norby, P., Hanson, J.C., 1998. In situ synchrotron X-ray powder diffraction studies of crystallization of microporous aluminophosphates and Me^{2+}-substituted aluminophosphates. Chem. Mater. 10, 1688–1693.

Cruciani, G., Artioli, G., Gualtieri, A., Stahl, K., Hanson, J.C., 1997. Dehydration dynamics of stilbite using synchrotron X-ray powder diffraction. Am. Mineral. 82, 729–739.

Davison, W., 1991. The solubility of iron sulfides in synthetic and natural waters at ambient temperature. Aquat. Sci. 53, 309–329.

de Moor, P.P.E.A., Beelen, T.P.M., Komanschek, B.U., Diat, O., Santen, R.A.v., 1997. In situ investigation of Si-TPA-MFI crystallization using (ultra-) small- and wide- angle X-ray scattering. J. Phys. Chem. B 101, 11077–11086.

Drobner, E., Huber, H., Wächtershäuser, G., Rose, D., Setter, K.O., 1990. Pyrite formation linked with hydrogen evolution under anaerobic conditions. Nature 346, 742–744.

Evans, J.S.O., Francis, R.J., O'Hare, D., Price, S.J., Clark, S.M., Gordon, J., Nield, A., Tang, C.C., 1994. An apparatus for the study of the kinetics and mechanism of hydrothermal reactions by in situ energy dispersive X-ray diffraction. Rev. Sci. Instrum. 66 (3), 2442–2445.

Francis, R.J., O'Hare, D., 1998. The kinetics and mechanisms of the crystallization of microporous materials. J. Chem. Soc., Dalton Trans., 3133–3148.

Furukawa, Y., Barnes, H.L., 1995. Reactions forming pyrite from precipitated amorphous ferrous sulfate. In: Vairavamurthy, M.A., Schoonen, M.A.A. (Eds.), Geochemical Transformations of Sedimentary Sulfur. ACS Symposium Series 612 American Chemical Society, Washington, DC, pp. 194–205.

Grey, C.P., Poshni, F.I., Gualtieri, A.F., Norby, P., Hanson, J.C., Corbin, D.R., 1997. Combined MAS NMR and X-ray powder diffraction structural characterization of hydrofluorocarbon-134 adsorbed on zeolite Na–Y: observation of cation migration and strong sorbate–cation interactions. J. Am. Chem. Soc. 119, 1981–1989.

Gualtieri, A., Norby, P., Hanson, J.C., Hriljac, J., 1996. Rietveld refinement using synchrotron X-ray powder diffraction data collected in transmission geometry using an imaging-plate detector: application to standard *m*-ZrO_2. J. Appl. Crystallogr. 29, 707–713.

Lee, Y., Cahill, C.L., Hanson, J.C., Parise, J.B., Carr, S.W., Myrick, M.L., Preckwinkel, U.V., Phillips, J.C., 1998. Characterization of K^+ ion exchange into Na-MAX using time resolved synchrotron X-ray powder diffraction and Rietveld refinement. In: Treacy, M.M.J. (Ed.), Proceedings of the 12th International Zeolite Conference, Baltimore, MD, USA.

Lennie, A.R., Redfern, S.A.T., Champness, P.E., Stoddart, C.P., Schofield, P.F., Vaughan, D.J., 1997. Transformation of mackinawite to greigite: an in situ X-ray powder diffraction and transmission electron microscopy study. Am. Mineral. 82, 302–309.

Luther, G.W. III, 1991. Pyrite synthesis via polysulfide compounds. Geochim. Cosmochim. Acta 55, 2839–2849.

Norby, P., 1996. In situ time resolved synchrotron powder diffraction studies of syntheses and chemical reactions. Mater. Sci. Forum 228–231, 147–152.

Norby, P., 1997a. Hydrothermal conversion of zeolites: an in situ synchrotron X-ray powder diffraction study. J. Am. Chem. Soc. 119, 5215–5221.

Norby, P., 1997b. Synchrotron powder diffraction using imaging plates; crystal structure determination and Rietveld refinement. J. Appl. Crystallogr. 30, 21–30.

Parise, J.B., Schoonen, M.A.A., Lamble, G., 1994. An extended X-ray absorption fine structure (EXAFS) spectroscopic study of amorphous FeS. Abstr. Geol. Soc. Am. 22, A293.

Parise, J.B., Weidner, D.J., Chen, J., Liebermann, R.C., Chen, G., 1998. In situ studies of the properties of materials under high-pressure and temperature conditions using multi-anvil apparatus and synchrotron X-rays. Annu. Rev. Mater. Sci. 28, 349–374.

Price, S.J., O'Hare, D., Francis, R.J., Fogg, A., O'Brien, S., 1996. Formation of surfactant intercalates of $MnPS_3$ as observed by real time in situ powder X-ray diffraction. Chem. Commun., 2453–2454.

Rickard, D.T., 1969. The chemistry of iron sulfide formation at low temperatures. Stockholm Contrib. Geol. 20, 67–95.

Rickard, D.T., 1975. Kinetics and mechanism of pyrite formation at low temperatures. Am. J. Sci. 275, 636–652.

Rickard, D.T., 1995. Kinetics of FeS precipitation: Part I. competing reaction mechanisms. Geochim. Cosmochim. Acta 59, 4367–4379.

Rickard, D.T., 1997. Kinetics of pyrite formation by the H_2S oxidation of iron(II) monosulfide in aqueous solutions between 25 and 125°C: the rate equation. Geochim. Cosmochim. Acta 61 (1), 115–134.

Rietveld, H.M., 1969. A profile refinement method for nuclear and magnetic structures. J. Appl. Crystallogr. 2, 65–71.

Rivers, M.L., Duffy, T.S., Wang, Y., Eng, P.J., Sutton, S.R., Shen, G., 1998. A new facility for high-pressure research at the advanced photon source. In: Properties of Earth and Planetary Materials at High Pressure. Geophysical Monograph 101 American Geophysical Union.

Roberts, W.M.B., Walker, A.L., Buchanan, A.S., 1969. The chemistry of pyrite formation in aqueous solution and its relation to the depositional environment. Miner. Deposita 4, 18–29.

Schoonen, M.A.A., Barnes, H.L., 1991a. Reactions forming pyrite and marcasite from solution: I. Nucleation of FeS_2 below 100 C. Geochim. Cosmochim. Acta 55, 1495–1504.

Schoonen, M.A.A., Barnes, H.L., 1991b. Reactions forming pyrite and marcasite from solution: II. Via FeS precursors below 100°C. Geochim. Cosmochim. Acta 55, 1505–1514.

Shaw, S., Clark, S.M., Wang, Y., Henderson, C.M.B., Cahill, C.L., Parise, J.B., Benning, L.G., Rivers, M.L., Shen, G., 1998. In situ Hydrothermal Synthesis using 13 BM-D at the APS. Central Laboratory of the research Council, Daresbury Laboratory, Technical Report No. DL-TR-98-002.

Shaw, S., Henderson, C.M.B., Clark, S.M., this issue (a). Hydrothermal formation of the hydrated calcium silicates tobermorite and xonotlite; an in situ synchrotron study.

Shaw, S., Henderson, C.M.B., Clark, S.M., this issue (b). Dehydration/re-crystallization of hydrated calcium silicate minerals: an elevated temperature, in situ synchrotron SAXS/WAXS study.

Sweeney, R.E., Kaplan, I.R., 1973. Pyrite framboid formation: laboratory synthesis and marine sediments. Econ. Geol. 68, 618–634.

Taylor, P., Rummery, T.E., Owen, D.G., 1979a. On the conversion of mackinawite to greigite. J. Inorg. Nucl. Chem. 41, 595–596.

Taylor, P., Rummery, T.E., Owen, D.G., 1979b. Reactions of iron monosulfide solids with aqueous hydrogen sulfide up to 160°C. J. Inorg. Nucl. Chem. 41, 1683–1687.

Wächtershäuser, G., 1988. Pyrite formation — the first energy source for life: a hypothesis. Syst. Appl. Microbiol. 10, 207–210.

Wei, D.W., Osseo-Asare, K., 1995. Formation of iron monosulfide — a spectrophotometric study of the reaction between ferrous and sulfide ions in aqueous solutions. J. Colloid Interface Sci. 174 (2), 273–282.

Wilkin, R.T., Barnes, H.L., 1996. Pyrite formation by reactions of iron monosulfides with dissolved inorganic and organic sulfur species. Geochim. Cosmochim. Acta 60 (21), 4167–4179.

Wilkinson, A.P., Speck, J.S., Cheetham, A.K., Natarajan, S., Thomas, J.M., 1994. In situ X-ray diffraction study of crystallization kinetics in $PbZr_{1-x}Ti_xO_3$ (PZT, $x = 0.0$, 0.55, 1.0). Chem. Mater. 6, 750–754.